Journal of Fluorescence
https://doi.org/10.1007/s10895-021-02747-8

ORIGINAL ARTICLE

Photoinduced Electron Transfer Reactions of Water Soluble Porphyrins in Zeolite Environment

Kandavelu Velappan[1] · Renganathan Rajalingam[1] · Anbazhagan Venkattappan[2]

Received: 5 February 2021 / Accepted: 4 May 2021

Abstract

Excited state interactions of zeolite adsorbed porphyrins have been investigated by steady state luminescence quenching technique with certain antioxidants such as reduced glutathione, ascorbic acid and *L*-cysteine. The zeolite supported porphyrins, *meso*-tetra (*N*-methyl-4-pyridyl) porphyrin (H_2TMPyP^{4+}) and zinc tetra(*N*-methyl-4-pyridyl) porphyrin ($ZnTMPyP^{4+}$) were prepared and characterized by various techniques such as Diffuse Reflectance Spectra (DRS), Scanning Electron Microscope (SEM), powder X-Ray Diffraction (XRD) and BET surface area. The interaction of zeolites with porphyrins are shown to increase the lifetime of the singlet excited state of porphyrins and decays are biphasic in nature. The splitting of the emission band of porphyrins occurs in 1:1 glycerol: water solution due to the changes in the dielectric of the solvation sphere associated with porphyrin. The Stern-Volmer plots of I_0/I vs quencher concentration [Q] were linear in the whole range of [Q] used. These studies revealed the effective quenching for zinc porphyrin compared to free base porphyrin. The effect of quenchers and zeolite acidity has also been studied and the quenching rate constant (k_q) is found in the order of 10^9 M^{-1} s^{-1}. The quenching reaction obeys Rehm-Weller Equation and is shown to be due to thermodynamically favoured electron transfer from quenchers to the excited singlet state of porphyrins (reductive quenching).

Keywords Zeolite/Porphyrins · Electron transfer · Fluorescence · Antioxidants

Introduction

Photochemical studies of metalloporphyrins have been of great interest in fields extending from chemistry, biology, medicine to optoelectronics [1–3]. Metalloporphyrins are the active sites of numerous proteins whose functions range from oxygen transport and storage (hemoglobin, myoglobin) to electron transport (cytochrome c, cytochrome oxidase) to energy conversion (chlorophyll) [4, 5]. They are also used as photosensitizers for photodynamic therapy (PDT) of cancer [6, 7]. Water soluble porphyrins are also of much interest because of their ability to bind with DNA [8, 9], act as photosensitizers in photocatalytic water reduction, oxidation [10] and their potential use in photogalvanic cells [11]. The mechanistic understanding of the transfer of electrons, protons and hydrogen atoms is of greater importance since many photochemical and photobiological processes are based on these primary events. The investigations of the interactions of photoexcited singlet states of the porphyrins by artificial photosensitized electron-transfer reactions [12–16] are very important to mimic photosynthesis as a means of solar energy conversion and storage.

In homogeneous solution, the excited states of porphyrins are not sufficiently long-lived for electron transfer quenching. There are several studies on fluorescence quenching of the porphyrins by quinones and nitroaromatics in organic solvents [17, 18]. The oppositely charged energetic intermediates of the porphyrin and quinones, due to their electrostatic attraction, were found to result in considerable decrease in the efficiency of the photoprocess. Many different host systems have been successfully applied as a means of controlling the efficiency of energy storage by preventing rapid back electron transfer. The net photoionization efficiency in organic assemblies such as cyclodextrins [19], polyelectrolytes [20], colloids [21], charged micelles [22, 23], vesicles [24] and hydrophilic-

✉ Anbazhagan Venkattappan
anbu80@gmail.com

[1] School of Chemistry, Bharathidasan University, Tiruchirappalli, Tamil Nadu 620 024, India

[2] Department of Chemistry, Vinayaka Mission's Kirupananda Variyar Arts and Science College, Vinayaka Missions Research Foundation (Deemed to be University), Salem, Tamil Nadu 636 308, India

Published online: 02 August 2021

hydrophobic environments such as water-in-oil microemulsions [25] are typically higher than that in homogeneous solution, but the photoinduced radicals are not stable at room temperature. In some cases, the photoyields in organic assemblies are limited by the polarity and solubility of the photoactive molecules. Other investigators have explored the design of microheterogeneous assemblies such as zeolites [26] and silica gels [27] to achieve charge separation. Their cages and pores provide an appropriate microenvironment to retard back electron transfer and increase the lifetime of the photogenerated radicals ion intermediates. This has been accomplished in several cases where reactions between an uncharged substrate and/or quencher result in formation of charged products, one of which is selectively expelled or sequestered by the assembly. Picosecond transient absorption techniques were performed to probe the excited-state dynamics, revealing ultrafast charge separation (~4 ps) occurring from the donor segment to acceptor. Ultrafast transient absorption experiments allowed to identify the process of quenching of the Zn-porphyrin fluorescence as an efficient photoinduced electron transfer reaction between the cage porphyrin and the included NDI guest. The process occurs on fast and ultrafast time scales in the two complexes (1.5 ps and ≤ 300 fs) leading to a short-lived charge separated state (charge recombination lifetimes in the order of 30–40 ps) [28, 29].

Photoinduced electron transfer (PET) is one of the most important mechanisms for developing fluorescent probes and biosensors for antioxidants. Quantitative prediction of the quantum yields of these probes and sensors is crucial to accelerate the rational development of novel PET-based functional materials [30].

Antioxidants such as glutathione, ascorbic acid and *L*-cysteine play a vital role in medicine, biology, polymer chemistry, cosmetics and in food industry. By intercepting oxidizing species, predominantly reactive radicals, they prevent cellular damage and polymer or food degradation. It is very important to understand the bimolecular reaction kinetics by which antioxidants intercept reactive oxidizing species, as studied herein, is of utmost importance for modeling their actual activity and understanding the mechanism by which antioxidants act. The important aim in such research areas is the quantification of the reactivity of antioxidants [31].

In this paper, influence of the antioxidants on the fluorescence behaviour of excited state of porphyrins adsorbed in zeolites in 1:1 glycerol water medium are reported. The effect of sensitizers, quenchers and zeolite acidity has also been studied. The structures of porphyrins and quenchers used in this study are given in Scheme 1. The mechanism of quenching and the pathways have been analyzed in terms of singlet excited state porphyrin-quencher interaction. The formation of radical ion pairs will be a reason for fluorescence quenching.

Experimental Section

The tetra(4-pyridyl) porphyrin (TPyP), methyl-*p*-toluene sulfonate, dimethyl formamide, reduced glutathione, ascorbic acid, *L*-cysteine and glycerol, zinc acetate, dowex and sephadex were of high purity from Fluka or Aldrich and were used as received. The zeolite-Y (Si/Al: 2.3) was obtained from Mid-Century chemicals and the zeolite Y (Si/Al: 1.6) was prepared by the reported procedure [32]. X-Ray powder diffraction (XRD) pattern of the zeolite has excellent agreement with the calculated simulation of the XRD pattern for faujasite zeolite [33].

Preparation of Water Soluble Porphyrins

H_2TMPyP^{4+} and $ZnTMPyP^{4+}$ were synthesized by reported procedure [34]. H_2TMPyP^{4+} was prepared by methylation of TPyP (100 mg) with methyl-*p*-toluene sulfonate (500 mg) by refluxing overnight in dimethylformamide. Most of the dimethylformamide was removed by vacuum distillation and the solution was cooled until the precipitation of tosylate salt of H_2TMPyP^{4+} occurred. The solid was filtered, washed sparingly with cold acetone and air dried. The metal (Zn) insertion was carried out by dissolving H_2TMPyP^{4+} in water together with 5 fold excess of zinc acetate and stirring the solution overnight. The anion was exchanged by passing the solution through chloride ion enriched resin, subsequently purified with dowex or sephadex columns.

Preparation of Zeolite Adsorbed Porphyrins

The porphyrin sensitizers H_2TMPyP^{4+} and $ZnTMPyP^{4+}$ were adsorbed onto zeolite Y with varying Si/Al ratio (i.e., 2.3 and 1.6) by suspending 1 g of latter in 25 mL of water containing 2×10^{-5} M solution of porphyrin. After stirring overnight, the suspension was filtered and washed with water until the washings were colourless. The filtered porphyrin exchanged zeolite powder was washed in a soxhlet extractor with methanol to remove unbound porphyrin, if any and allowed to dry in air. Comparison of the filtered bathing solutions before and after equilibration, by UV-Vis spectroscopy, showed that the loading levels of H_2TMPyP^{4+} and $ZnTMPyP^{4+}$ were 0.5 to 1×10^{-5} mol/g zeolite. The observed porphyrin loadings correspond to approximately monolayer (10^{-10} mol cm^{-2}) coverage [35] of the particle external surface. The electrostatic interactions between the anionic aluminosilicate support and the cationic porphyrin molecules contribute to the successful adsorption of the complexes.

Analyses

Absorbance spectra were recorded using Hewlett Packard 8452A spectrophotometer and Diffuse Reflectance Spectra

Scheme 1 Structures of porphyrins and quenchers used in this study

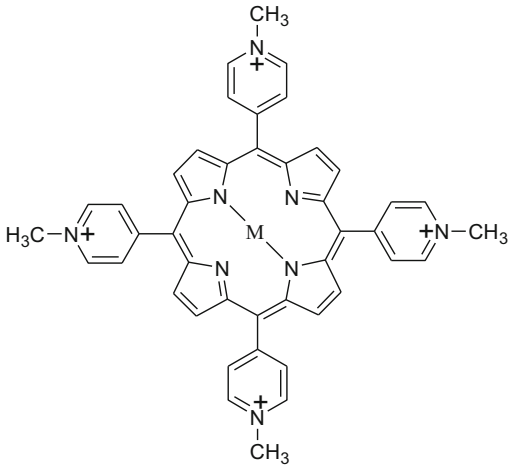

M = 2H H_2TMPyP^{4+}
M = Zn $ZnTMPyP^{4+}$

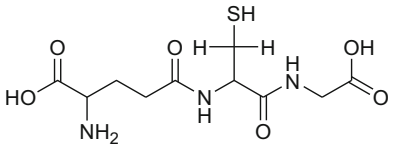

Reduced Glutathione

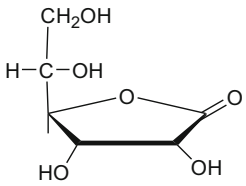

Ascorbic acid

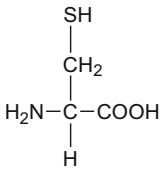

L-cysteine

(DRS) measurements were performed on CARY 5 UV-Visible spectrometer with an integrating sphere reflectance accessory. The X-Ray Diffraction (XRD) patterns of all the catalysts in this study were obtained on a Siemens D5000 X-ray diffractometer using Ni filtered Cu Kα radiation (λ = 1.5406) from 2θ = 20 to 60°. A conventional all glass volumetric high vacuum system was employed for the surface area measurements of the catalysts by nitrogen adsorption at liquid nitrogen temperature. Philips XL 30 SFEG instrument was employed for the Scanning Electron Microscope (SEM) measurement.

Fluorescence quenching experiments were carried out using a Perkin Elmer LS 50B spectrofluorimeter. The excitation wavelength was in all cases at or near the maximum of the Q(1,O) band of the porphyrins. The samples were dispersed by sonication in the desired medium. In the steady-state fluorescence measurements, a known amount of each porphyrin/zeolite sample was dispersed in 3 mL of the 1:1 glycerol: water solution with various concentrations of quenchers under nitrogen atmosphere and measurements taken at right angles in a 1 cm cuvette. The concentration of the quencher was normally of the order of 10^{-3} M to 0.1 M. Fluorescence lifetimes were measured with a PRA time-correlated single-photon counting system. Precautions were taken to eliminate spurious single photon counting data arising from scattering of the incident laser flash.

Results and Discussion

Absorption Studies

Absorption spectrum of H_2TMPyP^{4+} and $ZnTMPyP^{4+}$ in water are identical with those reported in the literature [34] showing the Soret band at 421 nm and 434 nm respectively. The shift of the electronic absorption spectra (Soret band) for metal porphyrin was closely connected to the electronegativity of the incorporated metal which strongly affects the π-electron system [36]. In 1:1 glycerol: water solutions, the three major absorption bands are red shifted approximately to 4 nm; adsorption onto the zeolite surface results in a further red shift of 2 nm in the Soret band and 2–4 nm in the Q bands. In terms of a band profile or shape, the Soret band is broadened by interaction with the zeolite. The shape of the spectra and band positions indicate the existence of the monomeric dye and non-occurrence of aggregation. The absorption spectra of zeolite adsorbed porphyrins were unaltered in the presence of quenchers. Kano et al. [37] reported the ground state complex formation for the H_2TMPyP^{4+} in the presence of AQDS by observing isosbestic point. The oxidation potential of the quencher used in our case ranges from −0.45 V to 0.35 V and if there is any ground state charge transfer (CT) complex formation, a new absorption peak should appear from the tail end of the H_2TMPyP^{4+} or $ZnTMPyP^{4+}$ absorption spectrum. This absorption shall be blue or red shifted depending on the oxidation potential of the quencher. The absence of any such absorption eludes the formation of the ground state complex.

Emission Studies

Emission spectrum of H_2TMPyP^{4+} and $ZnTMPyP^{4+}$ in water were identical with reported literature [34, 35]. As the porphyrins studied were free-base or closed shell metal porphyrin complexes, the fluorescent emission is attributed to the radiative deactivation of the electronic excited state associated with the porphyrin macrocycle. The emission of free-base porphyrins, like the optical absorption spectra, differ from metallic porphyrin emission due to the differences in their symmetries,

the former being significantly red shifted, i.e., the λ_{max} emission is 634 nm for $ZnTMPyP^{4+}$ whereas 685 nm for H_2TMPyP^{4+}. The change in the medium i.e., 1:1 glycerol: water medium, results in marked changes in the fluorescence emission spectrum of H_2TMPyP^{4+} and $ZnTMPyP^{4+}$. A blue shift of about 3–5 nm was observed for both porphyrins and the broad fluorescence band of porphyrins gives rise to two distinct bands, i.e., 680 nm and 725 nm for H_2TMPyP^{4+} from 685 nm, 630 nm and 672 nm for $ZnTMPyP^{4+}$ from 634 nm. The splitting of the emission band of H_2TMPyP^{4+} has been reported in methanol [34]. This effect is attributed to the changes in the dielectric of the solvation sphere associated with porphyrin. Adsorption onto the zeolite surface results further changes in the fluorescence excitation and emission spectrum of H_2TMPyP^{4+} and $ZnTMPyP^{4+}$. A red shift of about 6 nm in the excitation spectrum was observed for porphyrin-adsorbed zeolites when compared to the excitation spectrum of the free porphyrins. The shift in the emission maxima of 7–25 nm to lower wavelength (blue shift) was observed for both porphyrins adsorbed in zeolite. The broad fluorescence band of H_2TMPyP^{4+} shifts 20 nm and $ZnTMPyP^{4+}$ shifts 3 nm to lower wavelength from the fluorescence band observed in 1:1 glycerol: water. The observed broadening in the spectrum is expected due to the interaction with zeolites, which was observed in the case of $ZnTMPyP^{4+}$ and $ZnTAPP^{4+}$ on zeolite-L [31, 35]. The photophysical properties of H_2TMPyP^{4+}, $ZnTMPyP^{4+}$ in homogeneous solution and on zeolite with varying Si/Al ratio are summarized in Table 1.

Ground State Reflectance Spectra

The diffuse reflectance spectra (DRS) were examined to understand the presence and interaction of porphyrin with the zeolite. The UV-Vis DRS of zeolite-Y (Si/Al: 2.3) adsorbed H_2TMPyP^{4+}, $ZnTMPyP^{4+}$ are shown in Fig. 1**.** The presence of porphyrins was confirmed by the characteristic Soret band of H_2TMPyP^{4+} and $ZnTMPyP^{4+}$. Zeolite adsorbed porphyrins showed a red shift of about 6 nm (427 nm from 421 nm for H_2TMPyP^{4+} and 440 nm from 434 nm for $ZnTMPyP^{4+}$) in the Soret band when compared to the free porphyrins (not shown in figure). Broadening in the Soret band is expected due to interaction with zeolites. A similar observation was already observed in the case of $ZnTMPyP^{4+}$ and $ZnTAPP^{4+}$ adsorbed on zeolite–L [35]. The effects of Si/Al ratio and of the nature of the balancing cation seem to follow the acid-base properties of zeolites, indicating that the acid and basic sites are responsible for porphyrin adsorption.

BET Surface Area Measurements

Surface area measurements for the zeolite adsorbed porphyrins and bare zeolites give the information about the presence of porphyrin on the surface. The BET Surface area measurement for the zeolite adsorbed porphyrin catalysts is given in Table 2. The zeolite adsorbed porphyrins shows reduced surface area compared to bare zeolites. It could be due to the presence of porphyrins on the surface of zeolites.

Table 1 Physical properties of H_2TMPyP^{4+} and $ZnTMPyP^{4+}$ in water, 1:1 glycerol: water and on the zeolite-Y surface[d]

Property	H_2O	Glycerol	Zeolite-Y	
			Si/Al: 1.6	Si/Al: 2.3
H_2TMPyP^{4+}				
Electronic absorption wavelength maximum, nm	421 520 560 585	425 525 565 589	427 528 567 591	
Fluorescence emission wavelength maximum, nm	685	680 725	660 720	
τ_F/ns, fluorescence lifetime	5.3[a]	5.52	5.49 (77.32)[b] 9.54 (32.68)[c]	5.43 (60.90)[b] 8.75 (39.10)[c]
$ZnTMPyP^{4+}$				
Electronic absorption wavelength maximum, nm	434 560 600	438 562 602	440 566 606	
Fluorescence emission wavelength maximum, nm	634	630 672	627 670	
τ_F/ns, fluorescence lifetime	1.3[a]	1.53	1.45 (83.50)[b] 4.78 (16.50)[c]	1.41 (68.47)[b] 6.37 (31.53)[c]

[a] from ref. [3, 8], [b] fast component, [c] slow component, in 1:1 glycerol: water, biphasic decay, [d] Error limits: τ_F, ± 20%

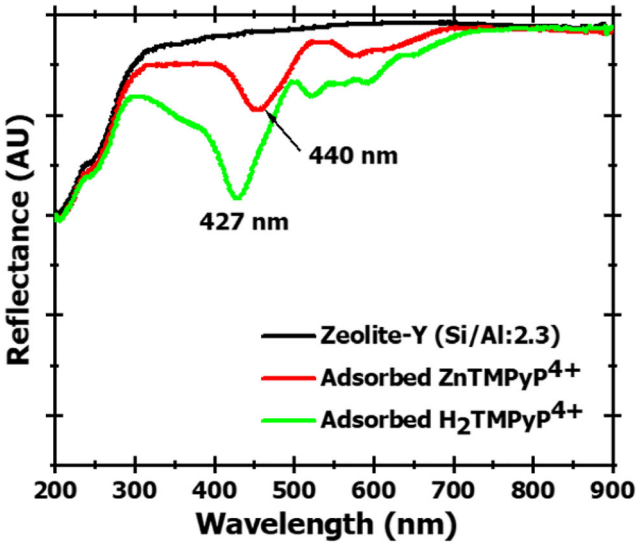

Fig. 1 UV-Vis diffuse reflectance spectra of zeolite-Y (Si/Al:2.3), adsorbed $ZnTMPyP^{4+}$ and H_2TMPyP^{4+}

X-Ray Diffraction Studies

X-ray powder diffraction permits one to ensure that the zeolite (host) crystallinity remains unaltered after its chemical modification. The X-ray powder diffraction patterns of H_2TMPyP^{4+} and $ZnTMPyP^{4+}$ loaded zeolites (Si/Al: 2.3 and 1.6) are presented in Fig. 2. None of the solids showed reduction in the intensity of peaks, suggesting the crystallinity retention of zeolite matrix. The main framework of the zeolite was not damaged. No variation was observed in the zeolite lattice parameters after the adsorption procedures.

SEM Analysis

The SEM image of porphyrin-zeolite-Y is similar to those observed for zeolite-Y, indicating that they possess the same morphology, i.e., the framework around the guest molecule porphyrin is zeolite-Y. A typical micrographs of zeolite (Si/Al: 1.6) adsorbed H_2TMPyP^{4+} were shown in Figs. 3 and 4. It suggests that the slid support is structurally unchanged and porphyrins should be dispersed molecularly on the external surface.

Table 2 Surface area of various zeolite-Y adsorbed porphyrins

Zeolite adsorbed porphyrin	Surface area ($m^2\ g^{-1}$)
Zeolite-Y (Si/Al: 2.3)	652
H_2TMPyP^{4+} / Zeolite -Y (Si/Al: 2.3)	640
$ZnTMPyP^{4+}$ / Zeolite -Y (Si/Al: 2.3)	642
Zeolite -Y (Si/Al: 1.6)	660
H_2TMPyP^{4+} / Zeolite -Y (Si/Al: 1.6)	645
$ZnTMPyP^{4+}$ / Zeolite -Y (Si/Al: 1.6)	650

Lifetime Measurements

To understand the role of zeolite and the solvent system, the singlet state lifetime (τ) of porphyrins in water, 1:1 glycerol water and zeolite adsorbed porphyrins system were measured and is shown in Table 1. The singlet state lifetime of H_2TMPyP^{4+} and $ZnTMPyP^{4+}$ in homogeneous condition is 5.3 ns and 1.3 ns respectively [34]. For 1:1 glycerol water system, the lifetime of the porphyrins increased by about ~0.2 ns. Fluorescence decays of porphyrins adsorbed on zeolites were biphasic in nature. The observed difference is due to the presence of zeolite environment and solvent used, which stabilizes the singlet lifetime of porphyrin and it varies with varying Si/Al ratio. The acid and basic sites present in zeolites are possibly responsible for the difference observed in lifetime. We can reason that the fast decay comes from a porphyrin ion which interacts strongly with the zeolite surface. This result suggests that singlet-state quenching of porphyrins by the quenchers may occur because of close positioning of the methyl pyridinium group of the two molecules.

Fluorescence Quenching

Fluorescence quenching of zeolite adsorbed porphyrin by various quenchers such as ascorbic acid, reduced glutathione and *L*-cysteine was carried out in 1:1 glycerol: water. The addition of quenchers did not change the porphyrin shape of fluorescence spectra and the absence of any new peak appearance eliminates the possibility of the ground state complex formation. Since there is no complexation between quencher and sensitizer, the water molecules from the solvation shell of the porphyrin remains as such. This, in effect, increases the possibility of collisional quenching of singlet excited state of porphyrins. The absence of CT complex absorption was already reported [38, 39] for the quenching of ionic porphyrin by neutral quenchers such as guanine and nitrobenzene. The concentration of quenchers used in this study is enough to quench the fluorescence of porphyrins. The emission intensity declines with the increase in the quencher concentration, which clearly indicates the quenching of porphyrin. Fluorescence quenching spectrum of zeolite-Y (Si/Al: 1.6) adsorbed H_2TMPyP^{4+} with various concentrations of ascorbic acid in 1:1 glycerol: water is shown in Fig. 5. The Stern-Volmer relationship was used for the analysis of fluorescence quenching [40].

$$I_0/I = 1 + K_{SV}\,[Q] \qquad (1)$$

where I_0 and I are the intensities of the fluorophore in the absence and the presence of quencher, respectively. K_{SV} is Stern-Volmer constant and [Q] is the concentration of the quencher.

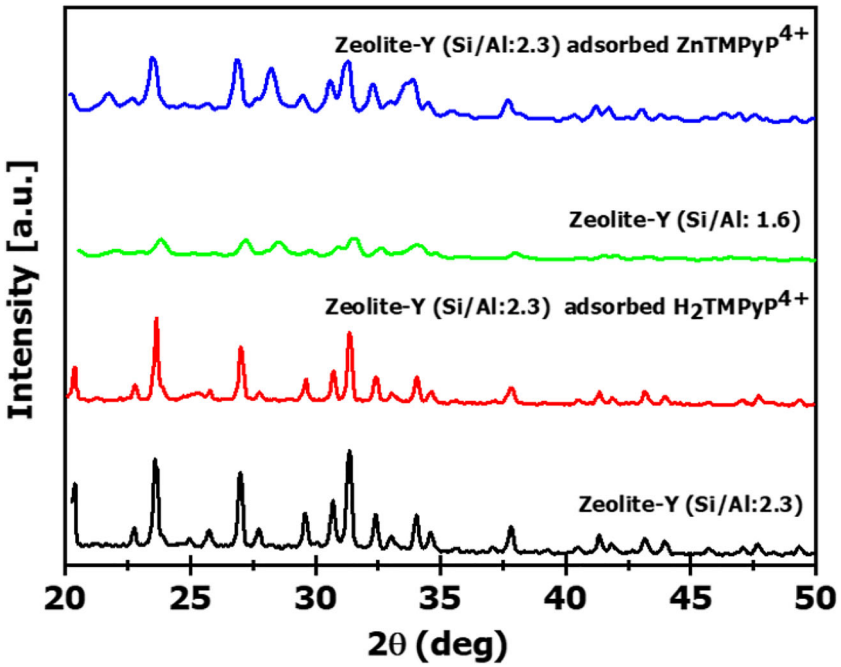

Fig. 2 Powder X-ray diffraction pattern of zeolite-Y (Si/Al:2.3), zeolite-Y (Si/Al:2.3) adsorbed H_2TMPyP^{4+}, zeolite-Y (Si/Al: 1.6) and zeolite-Y (Si/Al:2.3) adsorbed $ZnTMPyP^{4+}$

The bimolecular quenching rate constant, k_q was calculated using Eq. 2.

$$k_q = K_{SV}/\tau_0 \quad (2)$$

where τ_0 is the fluorescence lifetime of the porphyrin in the absence of quencher.

The Stern-Volmer plot of I_0/I versus [Q] yields a straight line for the porphyrin fluorescence quenching. In all the cases the correlation coefficient (r) is in the range of 0.99–0.97. A typical plot for the zeolite-Y (Si/Al: 1.6) adsorbed H_2TMPyP^{4+} with ascorbic acid is shown in Fig. 6. The process involves purely a dynamic quenching, i.e., quenching solely by collisional deactivation of the singlet excited state. The quenching rate constants for various zeolite adsorbed porphyrins with quenchers such as ascorbic acid, reduced glutathione and *L*-cysteine are shown in Table 3.

The k_q values observed for zeolite adsorbed H_2TMPyP^{4+} indicates that the quenching efficiency is more for reduced glutathione followed by ascorbic acid and *L*-cysteine. The same trend is observed for zeolite adsorbed $ZnTMPyP^{4+}$. This effect is due to better electron donating tendency of glutathione than other quenchers such as ascorbic acid and *L*-

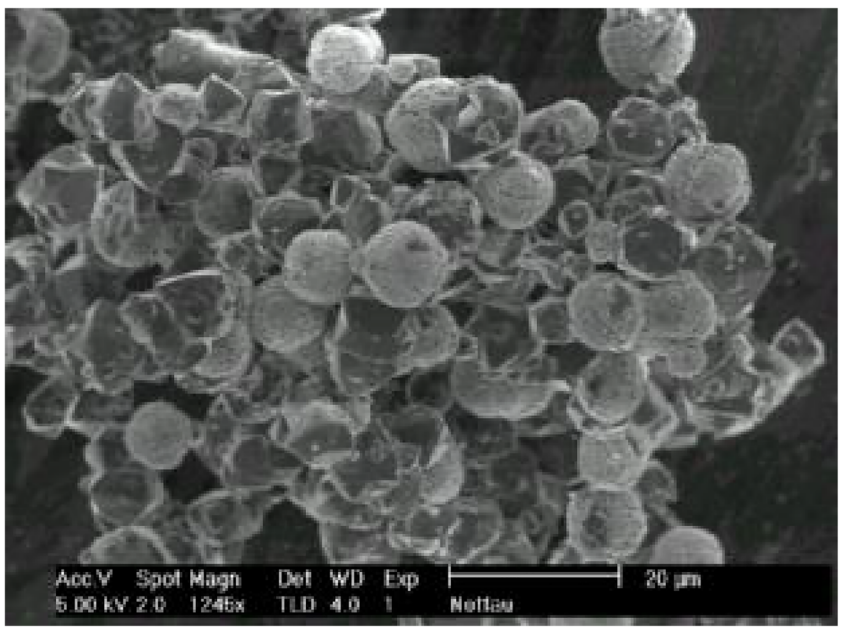

Fig. 3 Scanning electron microscope image of zeolite-Y (Si/Al: 1.6) adsorbed H_2TMPyP^{4+}

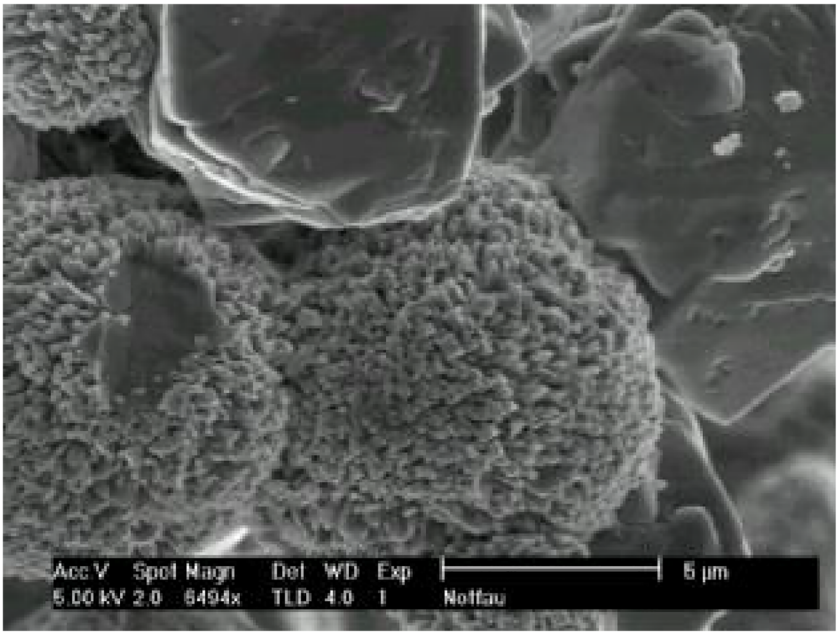

Fig. 4 Scanning electron microscope image of zeolite-Y (Si/Al: 1.6) adsorbed H_2TMPyP^{4+}

cysteine. The quenching of H_2TMPyP^{4+} is slower than its zinc complex, it is due to the fact that zinc complex is better oxidant than its free base porphyrin.

The dependence of k_q on zeolites reflects the influence of the difference in the structural features of the two different zeolites (Si/Al: 2.3 and 1.6) employed. The effects of Si/Al ratio and of the nature of the balancing cation, seem to follow the acid-base properties of zeolites, indicating that the acid and basic sites are possibly responsible for porphyrin adsorption and quenching. The strength of acid and basic sites is mainly determined by its cation nature, framework composition and the crystalline nature [41, 42]. For zeolite having Si/Al: 2.3 and 1.6, the difference is the framework composition. A richer aluminium zeolite (Si/Al: 1.6) will present a higher negative framework charge and a stronger basicity when the framework composition is concerned. So the strength of base sites is decreased in the order Si/Al: 1.6 > Si/Al: 2.3, while the Lewis acid strength is increased. Higher the acid strength, higher will be the quenching efficiency [43]. Due to the difference in the above properties, the quenching efficiency differs in the following order:

Porphyrin/zeolite − Y (Si/Al : 2.3) > Porphyrin/zeolite − Y (Si/Al : 1.6)

Quenching Mechanism

The quenching of porphyrins through electron transfer processes has been extensively studied. In number of systems net formation of products is observed when they possess the same charge. On the other hand, when an electron transfer process produces products with opposite charges, quenching of the excited state of the porphyrins leads to no net product formation.

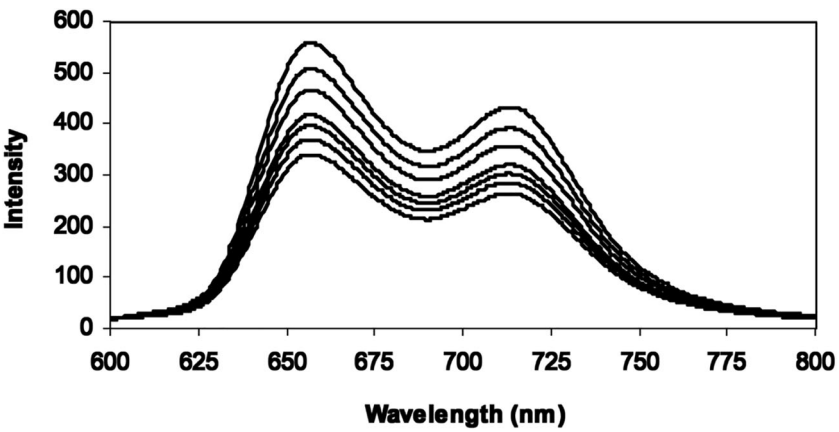

Fig. 5 Fluorescence quenching of zeolite-Y (Si/Al: 1.6) adsorbed H_2TMPyP^{4+} with various concentrations of ascorbic acid (0–9.75×10^{-3} M) in 1:1 glycerol: water

Table 3 Free energy change for electron transfer and quenching rate constant for the porphyrins in zeolites with various quenchers

Quencher	H_2TMPyP^{4+}			$ZnTMPyP^{4+}$		
	ΔG_{et} (eV)	k_q (10^9 M^{-1} s^{-1})		ΔG_{et} (eV)	k_q (10^9 M^{-1} s^{-1})	
		Z-Y(2.3)	Z-Y(1.6)		Z-Y(2.3)	Z-Y(1.6)
Reduced glutathione	−2.12	16.99	14.20	−1.48	52.05	48.27
Ascorbic acid	−1.42	15.30	11.76	−0.78	32.12	29.03
L-Cysteine	−2.22	2.96	2.55	−1.58	9.14	5.17

In the present system, only the porphyrin is being excited and the emission spectrum of porphyrin does not overlap with the absorption spectrum of the used quenchers. Therefore, energy transfer from H_2TMPyP^{4+} and $ZnTMPyP^{4+}$ to the quenchers cannot be acceptable mechanism for the quenching. Examination of redox potentials of the quenchers and the porphyrins demonstrate that the mechanism of singlet quenching most likely involves electron transfer between excited singlet of porphyrin and the quencher.

The nature of the electron transfer pathway (i.e., oxidative or reductive quenching of the porphyrin singlet state) can be understood by examining the free energy of the corresponding electron transfer reactions. The thermodynamics of electron transfer from the quencher to the porphyrin can be calculated by the well known Rehm-Weller equation [44].

$$\Delta G_{et} = E_{1/2(oxid.)} - E_{1/2(red.)} - E_{(0,0)} + C \quad (3)$$

where $E_{1/2(oxid.)}$ is the oxidation potential of the donor, $E_{1/2(red.)}$ is the reduction potential of the acceptor, $E_{(0,0)}$ is the singlet state energy of the sensitizer and C is the coulombic term. Since one of the species is neutral and the solvent used is polar in nature the coulombic term in the above expression is neglected [45].

The oxidation potential of reduced glutathione, *L*-cysteine and ascorbic acid are −0.35, −0.45 (vs HMDE) and 0.35 V (vs SCE) respectively [46–48]. The reduction potential of H_2TMPyP^{4+} and $ZnTMPyP^{4+}$ are - 0.23 V [49] and − 1.04 V [35] respectively, whereas the reduction potential changed significantly when they are exchanged into zeolite-Y showing a shift of both the metal and ring waves to more positive values by ca. 200 mV, i.e., − 0.06 V for H_2TMPyP^{4+} and - 0.85 V for $ZnTMPyP^{4+}$ [35]. The excited singlet state energy ($E_{(0,0)}$) for H_2TMPyP^{4+} is 1.83 eV and for $ZnTMPyP^{4+}$ is 1.98 eV. Thus, a thermodynamically favorable electron transfer from the quencher to the excited porphyrin will be anticipated only when $E_{1/2}(DH/DH^{\bullet+})$ is less than 1.77 and 1.13 V for H_2TMPyP^{4+} and $ZnTMPyP^{4+}$ respectively. All the quenchers used have less than that oxidation potential value, are expected to reduce the singlet excited state of porphyrins. The possibility of oxidative quenching (i.e., electron transfer from porphyrins to quenchers) can be eliminated due to the high electron donating ability and absence of electron accepting ability of quenchers. Thus it is suggested that observed quenching reaction involves electron transfer from quencher to porphyrin. The reduction of $ZnTMPyP^{4+}$ like that for H_2TMPyP^{4+} involve the formation of π-radical species,

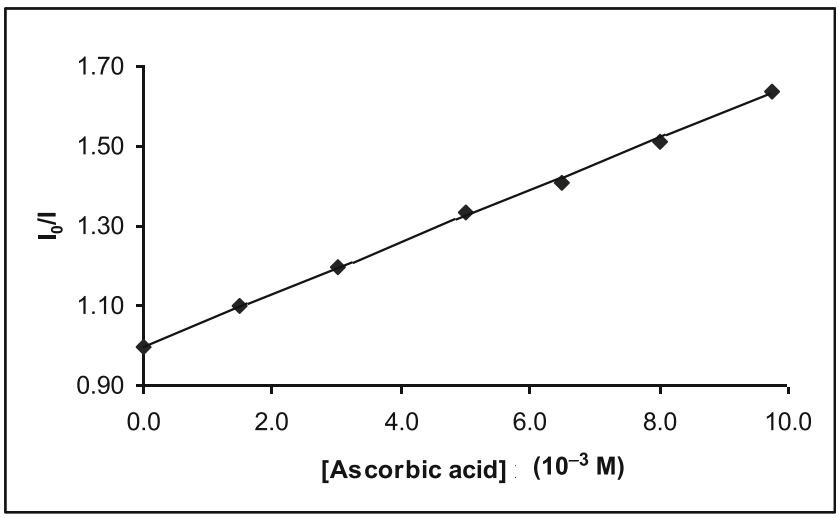

Fig. 6 Stern-Volmer plot for the fluorescence quenching of zeolite-Y (Si/Al: 1.6) adsorbed H_2TMPyP^{4+} with various concentrations of ascorbic acid (0–9.75×10^{-3} M) in 1:1 glycerol: water

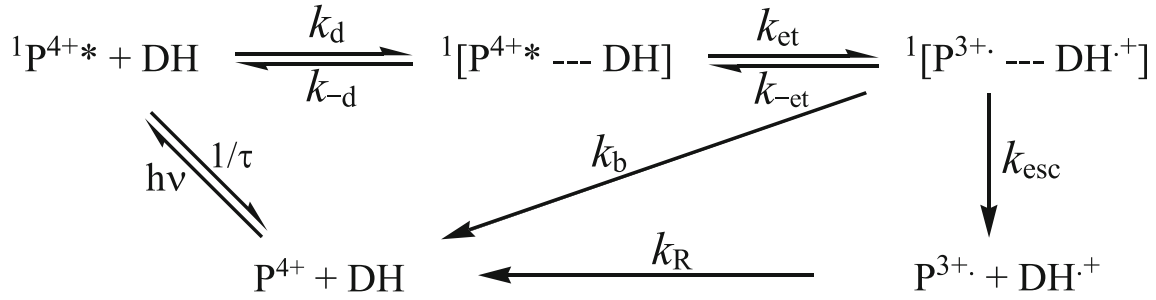

Scheme 2 Mechanism for the luminescence quenching of $P^{4+}*$ with DH

i.e., the metal ions are not readily reduced from the +2 state. Scheme 2 is proposed for electron transfer reaction in the present system.

In Scheme 2, P^{4+} and DH are porphyrins and quenchers respectively. k_d and k_{-d} are the rate constants of diffusion and dissociation coefficients of the encounter complex, respectively. k_{et} is the rate constant for the formation of radical ion pair and k_{-et} is the rate constant for the recombination. k_{esc} is the rate constant for the separation of the separated radical ion pair and k_R is the rate constant for the recombination of the separated radical ion pair. k_b is the rate constant for the charge recombination reaction producing the acceptor molecule in the ground state.

The radical ion pair either undergoes back electron transfer leading to regeneration of reactants or escape from the solvent cage to give the redox products (Eqs. 4 & 5).

$$DH^{\bullet+} \rightarrow D^{\bullet} + H^{+}, 2D^{\bullet} \rightarrow D\text{–}D \quad (4)$$

where DH = *L*-cysteine, reduced glutathione and ascorbic acid.

$$P^{3+\bullet} \rightarrow \text{disproportionation or protonation} \quad (5)$$

where $P^{4+} = H_2TMPyP^{4+}$ and $ZnTMPyP^{4+}$.

The quencher (DH) donates proton after the electron loss and it may be taken by the zeolite since it has the great affinity to take up the proton produced, by preventing the back electron transfer in heterogeneous system.

Conclusions

The presence of porphyrins on the surface and the crystallinity of zeolite were confirmed by DRS, BET surface area, XRD and SEM analysis. The interaction of zeolites with porphyrins increases the lifetime of the singlet excited state of porphyrins and decays are found to be biphasic. The splitting of the emission band of porphyrins occurs in 1:1 glycerol: water solution, similar to that observed for porphyrins in methanol which is attributed to the changes in the dielectric of the solvation sphere associated with porphyrin. In addition, the interactions cause the broadening of the spectrum. The data presented here demonstrate that the quenching of the singlet excited state of porphyrins, H_2TMPyP^{4+} and $ZnTMPyP^{4+}$ occurs in the presence of quenchers such as reduced glutathione, ascorbic acid and *L*-cysteine. Quenching studies revealed effective quenching for zinc porphyrin compared to free base porphyrin. Also quenching efficiency is more for glutathione than ascorbic acid and *L*-cysteine and zeolite-Y (Si/Al: 2.3) have high efficiency than zeolite-Y (Si/Al: 1.6). The decrease in fluorescence intensity of porphyrins with quenchers is now shown to be due to thermodynamically favoured electron transfer from quenchers to the excited singlet state of porphyrins (reductive quenching). The quenching reaction is shown to be with electron transfer rate on the order of 10^9 M^{-1} s^{-1}. Thus, zeolite-Y are found to be promising heterogeneous hosts for long lived photoinduced charge separation of adsorbed porphyrins.

Authors' Contributions AV and KV has carried out the experimental parts and prepared the draft of the manuscript. RR has contributed in the revision of the manuscript.

Funding No funding was received for conducting this study.

Data Availability All data generated or analysed during this study are included in this published article.

Code Availability Not applicable.

Declarations

Ethics Approval Not applicable.

Consent to Participate Not applicable.

Consent for Publications Not applicable.

Conflicts of Interest/Competing Interests Authors have no conflict of interest.

References

1. Grätzel M (1989) Heterogenous photochemical Electron transfer, 1st edn. CRC Press
2. Kalyanasundaram K (1987) Photochemistry in microheterogeneous systems. Elsevier
3. Müller-Dethlefs K, Hobza P (2000) Noncovalent interactions: a challenge for experiment and theory. Chem Rev 100:143–168. https://doi.org/10.1021/cr9900331
4. Milgrom LR (1997) The colours of life. An introduction to the chemistry of porphyrins and related compounds. Oxford University Press
5. Kadish KM, Smith KM, Guilard RBT-TPH (2003) The Porphyrin handbook. Elsevier
6. Dougherty TJ, Gomer CJ, Henderson BW, Jori G, Kessel D, Korbelik M, Moan J, Peng Q (1998) Photodynamic therapy. JNCI J Natl Cancer Inst 90:889–905. https://doi.org/10.1093/jnci/90.12.889
7. Bonnett R, Charlesworth P, Djelal BD, Foley S, McGarvey DJ, Truscott TG (1999) Photophysical properties of 5,10,15,20-tetrakis(m-hydroxyphenyl)porphyrin (m-THPP), 5,10,15,20-tetrakis(m-hydroxyphenyl)chlorin (m-THPC) and 5,10,15,20-tetrakis(m-hydroxyphenyl)bacteriochlorin (m-THPBC): a comparative study. J Chem Soc Perkin Trans 2:325–328. https://doi.org/10.1039/a805328f
8. Han FX, Wheelhouse RT, Hurley LH (1999) Interactions of TMPyP4 and TMPyP2 with Quadruplex DNA. Structural Basis for the differential effects on telomerase inhibition. J Am Chem Soc 121:3561–3570. https://doi.org/10.1021/ja984153m
9. Shimada E, Mori Y (2002) Photoinduced electron transfer of zinc porphyrin electrostatically bound to DNA. RIKEN Rev 46:22–23
10. Borgarello E, Kalyanasundaram K, Okuno Y, Grätzel M (1981) Visible light-induced oxygen generation and cyclic water cleavage sensitized by porphyrins. Helv Chim Acta 64:1937–1942. https://doi.org/10.1002/hlca.19810640626
11. Albery WJ (1982) Development of photogalvanic cells for solar energy conservation. Acc Chem Res 15:142–148. https://doi.org/10.1021/ar00077a003
12. Mandal H, Chakali M, Venkatesan M, Bangal PR (2021) Hot electron transfer from CdTe quantum dot (QD) to porphyrin and ultrafast electron transfer from porphyrin to CdTe QD in CdTe QD–Tetrakis(4-carboxyphenyl)porphyrin nanocomposites. J Phys Chem C 125:4750–4763. https://doi.org/10.1021/acs.jpcc.0c08229
13. Badgurjar D, Seetharaman S, D'Souza F, Chitta R (2021) One-photon excitation followed by a three-step sequential energy-energy-Electron transfer leading to a charge-separated state in a Supramolecular tetrad featuring Benzothiazole-boron-Dipyrromethene-zinc Porphyrin-C(60). Chem Eur J 27:2184–2195. https://doi.org/10.1002/chem.202004262
14. Koyuncu S, Hu P, Li Z, Liu R, Bilgili H, Yagci Y (2020) Fluorene–Carbazole-based porous polymers by photoinduced electron transfer reactions. Macromolecules 53:1645–1651. https://doi.org/10.1021/acs.macromol.9b02709
15. Nançoz C, Rumble C, Rosspeintner A, Vauthey E (2020) Bimolecular photoinduced electron transfer in non-polar solvents beyond the diffusion limit. J Chem Phys 152:244501. https://doi.org/10.1063/5.0012363
16. Wróbel D, Łukasiewicz J, Manikowski H (2003) Fluorescence quenching and ESR spectroscopy of metallic porphyrins in the presence of an electron acceptor. Dyes Pigments 58:7–18. https://doi.org/10.1016/S0143-7208(03)00032-9
17. Militello MP, Arbeloa EM, Hernández Ramírez RE, Lijanova IV, Montejano HA, Previtali CM, Bertolotti SG (2020) Photophysics and photochemistry of porphyrin core PAMAM dendrimers. Excited states interaction with quinones. J Photochem Photobiol A Chem 388:112167. https://doi.org/10.1016/j.jphotochem.2019.112167
18. Baird JK, Escott SP (1981) On departures from the Stern–Volmer law for fluorescence quenching in liquids. J Chem Phys 74:6993–6995. https://doi.org/10.1063/1.441074
19. Krishnan SB, Gopidas KR (2020) Generation of long-lived photo-induced charge separation in a supramolecular toroidal assembly. J Phys Chem B 124:9546–9555. https://doi.org/10.1021/acs.jpcb.0c05410
20. Koyama T, Sugiura J, Koishi T, Ohashi R, Asaka K, Saito T, Gao Y, Okada S, Kishida H (2020) Excitation energy transfer by electron exchange via two-step electron transfer between a single-walled carbon nanotube and encapsulated magnesium porphyrin. J Phys Chem C 124:19406–19412. https://doi.org/10.1021/acs.jpcc.0c06766
21. Willner I, Yang J-M, Laane C, Otvos JW, Calvin M (1981) The function of silicon dioxide colloids in photoinduced redox reactions. Interfacial effects on the quenching, charge separation, and quantum yields. J Phys Chem 85:3277–3282. https://doi.org/10.1021/j150622a014
22. Tutel Y, Sevinç G, Küçüköz B, Akhuseyin Yildiz E, Karatay A, Dumanoğulları FM, Yılmaz H, Hayvali M, Elmali A (2021) Ultrafast electron/energy transfer and intersystem crossing mechanisms in BODIPY-porphyrin compounds. Processes 9. https://doi.org/10.3390/pr9020312
23. Costa SMB, López-Cornejo P, Togashi DM, Laia CAT (2001) Photoinduced electron transfer in non-aqueous microemulsions. J Photochem Photobiol A Chem 142:151–161. https://doi.org/10.1016/S1010-6030(01)00509-3
24. Huo D, Peng Q, Xu T, Wang X, Wang X, Xia A, Lu R, Cui G, Wan Y (2020) Intramolecular energy transfer in a series of star-shaped molecules with a central porphyrin core and four oligocarbazole arms. J Phys Chem C 124:27356–27365. https://doi.org/10.1021/acs.jpcc.0c08451
25. Duan H, Cao F, Hao H, Bian H, Cao L (2021) Efficient photoinduced energy and electron transfers in a tetraphenylethene-based octacationic cage through host–guest complexation. ACS Appl Mater Interfaces 13:16837–16845. https://doi.org/10.1021/acsami.1c01867
26. Grätzel M, Kalyanasundaram K (eds) (1991) Kinetics and catalysis in microheterogeneous systems. CRC Press
27. Matsuura K, Kevan L (1996) Stabilization and electron spin resonance characterization of Ru(bpy)33+ in silica gel by chemical oxidation and photoinduced electron transfer. J Phys Chem 100:10652–10657. https://doi.org/10.1021/jp953078o
28. Jones AL, Jiang J, Schanze KS (2020) Excitation-wavelength-dependent photoinduced electron transfer in a π-conjugated Diblock oligomer. J Am Chem Soc 142:12658–12668. https://doi.org/10.1021/jacs.0c03678
29. Zanetti-Polzi L, Djemili R, Durot S, Heitz V, Daidone I, Ventura B (2020) Allosteric control of naphthalene Diimide encapsulation and Electron transfer in porphyrin containers: photophysical studies and molecular dynamics simulation. Chem A Eur J 26:17514–17524. https://doi.org/10.1002/chem.202003151
30. Chi W, Chen J, Liu W, Wang C, Qi Q, Qiao Q, Tan TM, Xiong K, Liu X, Kang K, Chang YT, Xu Z, Liu X (2020) A general descriptor ΔE enables the quantitative development of luminescent materials based on photoinduced electron transfer. J Am Chem Soc 142:6777–6785. https://doi.org/10.1021/jacs.0c01473
31. Köse ME, Schanze KS (2020) Prediction of internal reorganization energy in photoinduced electron transfer processes of molecular dyads. J Phys Chem A 124:9478–9486. https://doi.org/10.1021/acs.jpca.0c09533
32. Zhan B-Z, Li X-Y (1998) A novel 'build-bottle-around-ship' method to encapsulate metalloporphyrins in zeolite-Y. An efficient

biomimetic catalyst. Chem Commun:349–350. https://doi.org/10.1039/A706030K
33. Treacy MMJ, Higgins JB (2007) Collection of simulated XRD powder patterns for zeolites, Fifth Edit. Elsevier Science B.V
34. Kalyanasundaram K, Neumann-Spallart M (1982) Photophysical and redox properties of water-soluble porphyrins in aqueous media. J Phys Chem 86:5163–5169. https://doi.org/10.1021/j100223a022
35. Persaud L, Bard AJ, Campion A, Fox MA, Mallouk TE, Webber SE, White JM (1987) Photochemical hydrogen evolution via singlet-state electron-transfer quenching of zinc tetra(N-methyl-4-pyridyl)porphyrin cations in a zeolite L based system. J Am Chem Soc 109:7309–7314. https://doi.org/10.1021/ja00258a011
36. Murray RW (1984) Chemically modified electrodes. In: 'Electroanalytical chemistry, a series of advances. Marcel Dekker, New York
37. Kano K, Sato T, Yamada S, Ogawa T (1983) Fluorescence quenching of water-soluble porphyrins. A novel fluorescence quenching of anionic porphyrin by anionic anthraquinone. J Phys Chem 87:566–569. https://doi.org/10.1021/j100227a010
38. Magna G, Monti D, Di Natale C et al (2019) The assembly of porphyrin systems in well-defined nanostructures: an update. Molecules 24:4307. https://doi.org/10.3390/molecules24234307
39. Jasuja R, Jameson DM, Nishijo CK, Larsen RW (1997) Singlet excited state dynamics of Tetrakis(4-N-methylpyridyl)porphine associated with DNA nucleotides. J Phys Chem B 101:1444–1450. https://doi.org/10.1021/jp962684w
40. Stern O, Volmer M (1919) Uber die abklingungszeit der fluoreszenz. Phys Z 20:183–188
41. Huang M, Kaliaguine S (1992) Zeolite basicity characterized by pyrrole chemisorption: an infrared study. J Chem Soc{,} Faraday Trans 88:751–758. https://doi.org/10.1039/FT9928800751
42. Huang M, Adnot A, Kaliaguine S (1992) Characterization of basicity in alkaline cation faujasite zeolites—an XPS study using pyrrole as a probe molecule. J Catal 137:322–332. https://doi.org/10.1016/0021-9517(92)90160-J
43. Levin PP, Costa SMB, Lopes JM, Serralha FN, Ribeiro FR (2000) Effect of zeolite properties on ground-state and triplet-triplet absorption, prompt and oxygen induced delayed fluorescence of tetraphenylporphyrin at gas/solid interface. Spectrochim Acta Part A Mol Biomol Spectrosc 56:1745–1757. https://doi.org/10.1016/S1386-1425(00)00232-8
44. Rehm D, Weller A (1970) Kinetics of fluorescence quenching by Electron and H-atom transfer. Isr J Chem 8:259–271. https://doi.org/10.1002/ijch.197000029
45. Ramamurthy P, Parret S, Morlet-Savary F, Fouassier JP (1994) Spin—orbit-coupling-induced triplet formation of triphenylpyrylium ion: a flash photolysis study. J Photochem Photobiol A Chem 83:205–209. https://doi.org/10.1016/1010-6030(94)03826-0
46. Kizek R, Vacek J, Trnková L, Jelen F (2004) Cyclic voltammetric study of the redox system of glutathione using the disulfide bond reductant tris(2-carboxyethyl)phosphine. Bioelectrochemistry 63:19–24. https://doi.org/10.1016/j.bioelechem.2003.12.001
47. Heyrovský M, Mader P, Vavřička S, Veselá V, Fedurco M (1997) The anodic reactions at mercury electrodes due to cysteine. J Electroanal Chem 430:103–117. https://doi.org/10.1016/S0022-0728(97)00103-4
48. Mabbott GA (1983) An introduction to cyclic voltammetry. J Chem Educ 60:697. https://doi.org/10.1021/ed060p697
49. Nahor GS, Rabani J, Grieser F (1981) Properties of excited tetrakis(sulfonatophenyl)porphyrin in aqueous solutions. Photoredox reactions with quenchers. J Phys Chem 85:697–702. https://doi.org/10.1021/j150606a018